Sumer Journal for Pure Science (ISSN: 2790-7031)
SJPS 2026 (June), Vol. 5, No. 1, p.p.: 30-50

Green Synthesis of Silver Nanoparticles: Antimicrobial Efficacy against MDR Clinical Isolates and In Vitro Cytotoxicity Assessment

Sally R. Jwad

Department of Pathological Analyses, College of Science, University of Sumer, Thi-Qar, Iraq.
Email: sanhasr.alkafaji@gmail.com

Abstract

The environmental crises and rising multidrug -resistant (MDR) infections demand sustainable antimicrobial solutions. This study biosynthesized silver nanoparticles using Lactobacillus *plantarum* cell -free supernatant, characterized their physicochemical properties, and evaluated antimicrobial, antibiofilm, synergistic, and cytotoxic activityes against MDR clinical isolates from Iraq . AgNPs were synthesized via AgNO3 reduction and characterized using UV-Vis, FTIR,XRD, TEM, SEM, and zeta potential. Fifty isolates— including *Escherichia coli* , *Klebsiella pneumoniae* , *Staphylococcus aureus*, *Pseudomonas aeruginosa*, shigella spp., and NDM-1- positive strains— were obtained from Thi Qar, Iraq. UV-Vis confirmed bio reduction at 420 nm; XRD revealed 18 nm crystallite size; TEM/SEM showed uniform spherical morphology and zeta potential indicated colloidal stability. AgNPs exhibited potent bactericidal / bacteriostatic activity and 62-89% biofilm inhibition at sub- MIC concentrations. Synergistic effects with ampicillin and ciprofloxacin were confirmed via checkerboard assay. MTT assay demonstrated selective toxicity against human dermal fibroblasts. Biogenic AgNPs represent promising biocompatible alternatives for combating MDR infection, combining potent antimicrobial efficacy, antibiofilm activity, antibiotic synergy, and favorable safety profiles for clinical translation.

Keywords: Silver Nanoparticles, Multidrug Resistance, *Lactobacillus plantarum*, antimicrobial activity, and antibiofilm activity.

تخليق الجسيمات النانوية الفضية بالطرق الخضراء : الفعالية المضادة للميكروبات ضد عزلات سريرية ذات مقاومة متعددة للادوية وتقييم السمية الخلوية في المختبر

سالي ريسان جواد

قسم التحليلات المرضية، كلية العلوم، جامعة سومر، ذي قار، العراق

الخلاصة

تتطلب الازمة البيئية وتصاعد العدوى بالبكتريا متعددة المقاومة للمضادات حلولا مستدامة مضادة للميكروبات . هدفت هذه الدراسة لتصنيع جسيمات الفضة النانوية باستخدام الراشح الخلوي لبكتيريا *Lactobacillus plantarum*,وتوصيف خصائصها ,وتقييم فعاليتها المضادة للمكيروبات والاغشية الحيوية,وتاثيرها التازري مع المضادات الحيوية , وسميتها الخلوية ضد عزلات سريرية مقاومة .تم تصنيع جسيمات الفضة النانوية عن طريق اختزال نترات الفضة، وتم توصيفها باستخدام تقنيات الأشعة فوق البنفسجية والمرئية، والأشعة تحت الحمراء بتحويل فورييه، وحيود الأشعة السينية، والمجهر الإلكتروني النافذ و الماسح، وقياس جهد زيتا .جمعت خمسون عزلة – شملت الاشريكية القولونية ,الكليبسيلا الرئوية ,المكورات العنقودية ,الزائفة الزنجارية ,الشيغيلا ,وعزلات موجبة ل لـ-NDM 1من محافظة ذي قار.اكدت التحاليل الطيفية والمجهرية نجاح التصنيع الحيوي , وحجما بلوريا 18 نانو متر ,وشكلا كرويا منتظما(15-45نانومتر), وثباتا غرويا .اظهرت الجسيمات فعالية مبيدة ومثبطة للبكتريا ,وتثبيطا للاغشية الحيوية بنسبة 62-89%عند تراكيز دون المثبطة .واكدت اختبارات التازر فعالية تآزرية مع الامبيسلين والسيبروفلوكساسين.واظهر اختبار MTTسمية انتقائية ضد الخلايا الليفية الجلدية البشرية.تشكل الجسيمات النانوية الحيوية بدائل واعدة ومتوافقة حيويا لمكافحة العدوى متعددة المقاومة ,لجمعها بين الفعالية المضادة للميكروبات ,وتثبيط الاغشية الحيوية ,والتازر مع المضادات الحيوية , وقواعد امان مرغوبة للتطبيقات السريرية المستقبلية .

1. Introduction

The swift emergence and proliferation of multi-drug resistant (MDR) bacterial pathogens represent a formidable challenge to the advancements achieved over recent decades in the management of infectious diseases[1, 2].The World Health Organization has identified antimicrobial resistance (AMR) as a global priority, placing particular emphasis on MDR Gram-negative bacteria (such as carbapenem-resistant Enterobacteriaceae and Pseudomonas aeruginosa) as critical pathogens necessitating the urgent development of novel therapeutic interventions[3]. In Iraq, particularly within the Thi Qar Governorate, the issue of MDR bacterial infections has escalated significantly, with clinical isolates demonstrating resistance to a diverse array of antibiotics, including β-lactams, fluoroquinolones, aminoglycosides, and carbapenems[4],[5].

Numerous traditional antibiotics have lost their therapeutic efficacy due to various resistance mechanisms that have emerged, such as the production of extended-spectrum β-lactamases (ESBLs), carbapenemases (specifically New Delhi metallo-β-lactamase-1, NDM-1), and the overexpression of efflux pumps [6, 7]. The management of infections complicated by biofilm formation has become increasingly challenging due to the pathogens' interactions with the host immune response and their reactions to antimicrobial agents[8]. Organisms residing within biofilm structures exhibit a significantly greater (100-1000 times) resistance to antibiotics compared to their planktonic counterparts. Consequently, there is an urgent need for the development of novel and innovative strategies to effectively address these formidable infections [9, 10] .Silver nanoparticles in antimicrobial therapies that utilize novel discoveries in nanotechnology is positive development with the potential to interrupt structures in the bacterial cells (including membrane), disrupts other cells by releasing reactive oxygen species (ROS), and inhibits the processes DNA and protein synthesis, and others. These characteristics confirm that the likelihood developing immunities, including bacterial, would be greatly diminished. Thus, these nanoparticles prove to be AgNPs [11, 12]. Additionally, the combination of AgNPs and antibiotics has the potential to reduce antibiotic resistance and improve the efficacy of antimicrobial therapies[13-15]. The synthesis of AgNPs has been accomplished by conventional means (chemistry and physics) but includes risks related to toxicity and waste, complicating the application of these methods in the field of medicine. Utilizing biological systems such as plants, algae, and fungi is much safer and can be more cost-effective for medical applications [16, 17]. Probiotic bacteria, and particularly the strains of Lactobacillus, are biosafe, and as a result, the production of AgNPs by these bacteria Lactobacillus has been suggested. [18, 19]*Lattobacillus plantarum* has been identified as a probiotic that exists as a fermentant and in the intestines of humans. It has been documented that *L. plantarum* has the ability to produce a large and varied group of bioactive compounds that include organic acids, bacteriocins and a number of bioactive reductive and capping enzymes. The cell free supernatant of *L. plantarum* contains an abundance of bioactive proteins and enzymes and other secondary metabolites that aid in the reduction of silver ions (Ag^{+}) to elemental silver (Ag^{0}) while also providing bioactive capping that shields from aggregation and improves biocompatibility. The antimicrobial activity of Lactobacillus, against a number of pathogenic microorganisms, and the silver nanoparticles (AgNPs) has been documented in many publications. However, the authors are not aware of the reports on multi-drug resistant (MDR) clinical isolates from a particular geographic area, Iraq, and the various studies that are available.

This study attempts to identify an area of this gap in research by analyzing the environmentally acceptable construction of AgNPs using the cell-free supernatant of *L. plantarum* along with the complete physicochemical characterization combined with the thorough systematic antimicrobial spectrum of multidrug resistant (MDR) clinical isolates which were collected from the first line health care centres in Thi Qar Governorate, Iraq, Research Antibacterial. Furthermore, this research will attempt to assess the anti-biofilm activity, the cytotoxicity to human dermal fibroblasts, the synergism with the standard antibiotics (ciprofloxacin, ampicillin) and the in silico molecular docking studies in order to determine the

molecular consequences of the thing that is caused by the infection. The combination of nano-technology, microbiology, and computer science will provide a comprehensive approach to the use of biogenically synthesized AgNPs to solve the growing problem of clinical multidrug resistance.

2. Materials and Methods

2.1 Bacterial Strain and Culture Conditions

The American Type Culture Collection (ATCC, Manassas, VA, USA) maintains Lactobacillus plantarum (ATCC 8014) as a glycerol stock at -80 ℃. The strain was cultivated in a de Man, Rogosa, and Sharpe (MRS) broth (Oxoid, UK) at 37 °C for 24 hours under microaerophilic conditions. Purity testing was performed by Gram's method, catalase activity, and 16S rRNA gene sequencing.

2.2 Preparation of Cell-Free Supernatant

Lactobacillus Plantarum was inoculated and grown in 500 mL of MRS broth for 48 hours at 37 °C in an orbital shaker at 120 rpm. After incubation, the culture was centrifuged at 10,000 rpm for 15 minutes at 4 °C. The cell-free supernatant was filtered using Millipore, USA 0.22 µm cellulose acetate membrane filter to remove remaining bacterial cells and cell debris. The supernatant was kept at 4 °C and used for nanoparticle synthesis within 72 hours[20].

2.3 Eco-Friendly Synthesis of Silver Nanoparticles

Since AgNPs were synthesized, silver nitrate ($AgNO_3$, 99.9% purity, Sigma-Aldrich, USA) was added to cell-free supernatant. A total of 10 mL of 10 mM $AgNO_3$ was added to a 250 mL Erlenmeyer flask containing cell free supernatant. In total, 90 mL cell free supernatant was mixed with 10 mL of 10 mM $AgNO_3$ to make a final concentration of 1 mM of $AgNO_3$. The final mixtures were incubated at 37 degrees Celsius in a dark cupboard while stirring at 150 rpm for 72 hours. The initially pale yellow of Ag^+ ions started to become a deep brown color, which indicated the presence of AgNPs. Control experiments were performed using MRS broth without bacterial supernatant and $AgNO_3$ to determine the function of bacterial supernatant in nanoparticle synthesis [21, 22]

AgNPs were isolated by centrifugation at 15,000 rpm for 20 minutes. To remove any bound biological materials, and silver ions, AgNPs were washed three times with sterilized distilled water. AgNPs after purification were re suspended in sterilized distilled water and lyophilized using a freeze dryer (Christ Alpha 1-2 LD Plus, Germany) to prepare a dry powder form for biological assays and characterization. The AgNPs after lyophilization were kept in amber vials to protect from light and at 4 degrees Celsius .

2.4 Characterization of AgNPs

2.4.1 UV-Visible Spectroscopy

In this study, we used UV-Visible spectrophotometry (Shimadzu UV-1800, Japan) in the range of 300-700 nm to evaluate the formation and stability of silver nanoparticles (AgNPs). The samples were properly diluted, and in order to determine the surface plasmon resonance (SPR) peak that is characteristic of AgNPs, the absorbance spectra were recorded daily for 24 hours during the synthesis. [23]

2.4.2 Fourier-Transform Infrared Spectroscopy (FTIR)

FTIR is used for signature identification of functional groups concerning the bioreduction and stabilization processes of silver nanoparticles (AgNPs). A sample of lyophilized AgNPs was prepared in

synergy with potassium bromide (KBr) in a 1:100 ratio and then pressed into a pellet for analysis in the spectral range of 4000 to 400 cm^{-1} and a resolution of 4 cm^{-1} (Bruker Tensor 27, Germany) .

2.4.3 X-Ray Diffraction (XRD):

The crystal structure of the AgNPs was investigated using x-ray diffraction (Rigaku MiniFlex 600, Japan) with Cu Kα radiation (λ = 1.5406 Å) operated at 40 kV and 15 mA. Diffraction patterns were collected in the 2θ range of 20 to 80° with the scanning speed of 2° min^{-}. The average crystallite size was calculated using the Debye-Scherrer formula:

$$D = K\lambda / (\beta \cos \theta)$$

Here, D = the crystallite size, K = shape factor (0.9), λ = the X-ray wavelength, β = the full width at half maximum (FWHM) of the diffraction peak, and θ = the Bragg angle [24].

2.4.4 Transmission Electron Microscopy (TEM) and Scanning Electron Microscopy (SEM)

The morphology and size uniformity of the synthesized silver nanoparticles, were measured using Transmission Electron Microscopy (TEM) (JEOL JEM-2100, Japan) at an accelerating voltage of 200 kV. A drop of the diluted AgNP suspension was cast on a carbon-coated grid and the solvent was allowed to evaporate, to prepare the sample. The size distribution was studied by measuring at least 200 particles by the software Image J (NIH, USA). The SEM (FEI Quanta 250 FEG, USA) technique was also used to study the surface morphology and agglomeration of the sample [25].

2.4.5 Zeta Potential Analysis

Using the Zetasizer Nano ZS (Malvern Instruments, UK) for electrokinetic light scattering, we evaluated the surface charge and colloidal stability of the silver nanoparticles (AgNPs) via the zeta potential. The measurements were done in triplicate at 25°C using a dilution of deionized water .

2.5 Collection of Clinical Samples

Esteemed ethics subcommittees of the University of Sumer (Approval Number UTQ-MED-2023-045) authorized this research. From January 2024 to June 2024, 50 samples were collected from patients with clinically diagnosed bacterial infections at Al-Hussein Teaching Hospital and Al-Nasiriyah General Hospital in the Thi Qar Governorate, Iraq. Sample type distribution included urine (n=18), wound swab (n=15), blood culture (n=10), and sputum (n=7) samples. Participants and/or their legally authorized representatives provided informed consent. Clinical and demographic information were recorded thoroughly. Sample transport to the microbiology lab occurred within two hours of collection and were appropriately immobilized.

2.6 Isolation and Identification of Bacterial Isolates

The clinical samples were dealt with in the manner prescribed for microbiological specimens. The samples were inoculated onto both selective and differential culture media of MacConkey, Blood, Mannitol Salt, and Eosin Methylene Blue Agars (all from Oxoid, UK) and incubated at 37 °C. A range of 24-48 hours was used for the incubation. Bacterial isolates were classified as one of many possible types based on how the colonies looked (i.e. colony morphology) and the results of some tests (e.g. Gram staining, catalase, oxidase, indole, methyl red, Voges-Proskauer, citrate utilization, urease, and triple sugar iron tests). The VITEK 2 Compact automated system (bioMérieux, France) was used for the identification of species, at the level of species, employing GN and GP identification cards .

2.7 Antimicrobial Susceptibility Testing

Clinical isolate profiles were drawn for susceptibility to antimicrobials using the Kirby-Bauer technique. Bacteria cultured to the 0.5 McFarland standard were spread evenly over Mueller-Hinton (M-H) Agar plates. The paraffin discs were dispensed on the agar surface, and included, ampicillin (10 µg), amoxicillin-clavulanic acid (20/10 µg), ceftriaxone (30 µg), ceftazidime (30 µg), ciprofloxacin (5 µg), levofloxacin (5 µg), gentamicin (10 µg), amikacin (30 µg), imipenem (10 µg), meropenem (10 µg), and colistin (10 µg). The plates were incubated for 37o C for 18 to 24 hours, and the measurement for the diameter of the inhibition zone was done, and classified based on the CLSI breakpoints. Isolates that were resistant to three or more classes of antibiotics were categorized as multidrug-resistant .

The presence of carbapenemase was determined using the modified Hodge test and a phenotypic confirmatory test using EDTA and boronic acid. The NDM-1 gene was detected by polymerase chain reaction (PCR) using pre-designed specific primers (Forward: 5'-GGTTTGGCGATCTGGTTTTC-3';Reverse: 5'-CGGAATGGCTCATCACG-ATC-3')[26].

2.8 Evaluation of MIC and MBC:

Using broth microdilution method, assessing Minimum Inhibitory Concentration (MIC) and Minimum Bactericidal Concentration (MBC) of silver nanoparticles (AgNPs) against multidrug-resistant (MDR) isolates was conducted in compliance with Clinical and Laboratory Standards Institute (CLSI) and 96 well microtiter plates. AgNps stock solutions of 1000 µg/mL concentration were prepared in sterile, distilled water and also in two-fold serial dilution in cation-adjusted Mueller Hinton broth (CAMHB) to obtain final concentration range of 0.78 - 100 µg/mL. With respect to 0.5 McFarland (approx. 1.5 x 10^8 CFU/mL) bacterial suspension, 1:100 dilution was done in CAMHB and 100 µL of this dilution was added to each well containing 100 µL of AgNPs to achieve final inoculum of 5 x 10^5 CFU/mL. The plates were incubated at 37 degrees celsius for 18-24 hours. MIC is defined as the lowest concentration showing no growth of bacterial cultures. For growth of MBC, 10 µL sample was transferred from no growth bacterial well to Mueller Hinton Agar (MHA) plates, incubated at 37 degrees celsius for 24 hours. For this study, the MBC is considered lowest concentration resulting in bacterial viability 99.9% or greater. Experimental procedures were conducted in triplicate [27, 28]

2.9 Evaluation of Anti-Biofilm Efficacy

The ability to inhibit the formation of biofilms was evaluated using a crystal violet assay. This assessment was done using silver nanoparticles (AgNPs) and 96-well flat bottom polystyrene microtiter plates. As per the 0.5 McFarland standard, bacterial suspensions were diluted 1:100 in tryptic soy broth (TSB) with 1% glucose. To each well of the microtiter plate containing 200 µL of the bacterial suspension, AgNPs were added at concentrations of 1/2 MIC, 1/4 MIC, and 1/8 MIC. The plates were then incubated at 37°C for 24 hours under static conditions for biofilm formation. After the 24-hour incubation, planktonic cells were removed by washing 3 times with sterile phosphate buffered saline (PBS, pH 7.4). The adhered biofilm was then fixed with 200 µL of 99% methanol for 15 min, allowed to air dry, and was then treated with 200 µL of 0.1% crystal violet stain for 20 min. The stain was removed with distilled water. Any crystal violet stain that remained was solubilized with 200 µL of 33% glacial acetic acid. Absorbance was measured at 570 nm using a microplate reader (BioTek ELx800, USA). The biofilm inhibition was calculated using the formula:

Biofilm Inhibition (%) = $[(OD_{570}$ control - OD_{570} treated) / OD_{570} control$] \times 100$

All experiments were done in triplicate and contained appropriate controls [29, 30]

2.10 Evaluating Antibiotic Synergism

Using the microdilution checkerboard method, we evaluated the synergism of three antimicrobial properties of silver nanoparticles (AgNPs) combined with two antibiotics (ciprofloxacin and ampicillin). In a 96-well microtiter plate, a two-dimensional grid was formed, where the dilutions of AgNPs (from 1/8 of the Minimum Inhibitory Concentration (MIC) to 2 × MIC) were positioned along one axis, and antibiotics were positioned along the orthogonal axis. Into each well, 100 µL of a bacterial suspension (5×10^5 colony-forming units (CFU)/mL) was added, and then incubated for 18–24 hours at 37 °C. The Fractional Inhibitory Concentration (FIC) Index was then calculated using this formula:

FIC Index = (MIC of AgNP in combination / MIC of AgNP alone) + (MIC of antibiotic in combination / MIC of antibiotic alone)

FIC Index values for synergy and antagonism were 0.5 and > 4.0, respectively. The terms additive and indifferent were used to describe $0.5 <$ FIC Index ≤ 1.0 and $1.0 <$ FIC Index ≤ 4.0, respectively. All experimental procedures were conducted in triplicate as per [31].

2.11 Cytotoxicity Assay

The cytotoxicity of silver nanoparticles (AgNPs) on human dermal fibroblast (HDF) cells (ATCC PCS-201-012) was tested using MTT cytotoxicity assay. HDF cells were grown in Dulbecco's Modified Eagle Medium (DMEM, Gibco, USA) with 10% fetal bovine serum (FBS) and antibiotics (penicillin 100 U/mL and streptomycin 100 mg/mL) and kept in an incubator at 37°C with 5% CO_2. For the test, 10,000 HDF cells were plated in 96 well plates and allowed to adhere for 24 hours. The HDFs were then exposed to formulated AgNPs in complete assay medium at concentrations of 3.125 to 200 µg/mL in triplicates. After 24 hours exposure, 20 µL of MTT solution (5 mg/mL in PBS) was added to each well, and the cells were incubated for another 4 hours at 37°C. The medium was removed, taking care to leave the cells, and 150 µL of dimethyl sulfoxide (DMSO) was added to dissolve the formazan crystals. The absorbance was measured at 570 nm using a microplate reader. The cytotoxicity of the particles was calculated using the following equation:

Cell viability (%) = (OD_{570} treated / OD_{570} control) × 100 The IC_{50} was determined using non-linear regression in GraphPad Prism Software (version 9.0).

2.12 Molecular Docking Studies

AgNPs with bacterial membrane proteins interaction mechanisms were explored via Molecular Docking Studies. The Protein Data Bank was used to access the relevant target proteins, OmpA from Escherichia coli (PDB ID: 1QJP), penicillin-binding protein 2a (PBP2a) from Staphylococcus aureus (PDB ID: 3ZG0) and from Pseudomonas aeruginosa (PDB ID: 2LHF) OprF. The protein structures were processed using AutoDock Tools version 1.5.6 by removing water molecules, adding the polar hydrogen atoms and specifying Kollman charges. The silver nanoparticle aggregates (Ag_{13}) were created and energy minimized on the Avogadro platform. Molecular Docking was performed using AutoDock Vina with the active site defined by a grid box of dimensions 40 x 40 x 40 Å with 0.375 Å spacing. Exhaustiveness was set to 8, and binding energy (kcal/mol) calculations were performed on the poses that were deemed top-ranking. PyMOL and Discovery Studio Visualizer were used to analyze and visualize the protein-ligand interactions [32, 33]

2.13 Statistical Analysis

All experiments were done in triplicate and results expressed as mean ± standard deviation (SD). For statistical analysis, IBM SPSS Statistics (Version 26.0, IBM, USA) was used. For comparison of means in multiple groups, one-way analysis of variance (ANOVA) was used, followed by Tukey's post hoc test. For

comparison of means in two groups, Student's t-test was used. For all statistical analyses, a p value < 0.05 was considered significant. Data plots were generated using GraphPad Prism version 9.0.

3. Results

3.1 Synthesis and Characterization of AgNPs

3.1.1 Visual Observation and UV-Visible Spectroscopy

One of the most convincing signs of bio reduction of silver ions by L. plantarum cell-free supernatant was the change of colour from pale yellow to deep brown. This change was observed for the period of 24 hours. The deep brown colour continued to increase for 72-hour incubation period. The increased brown color indicates the increased of surface plasmon resonance (SPR) of silver nanoparticles. The UV-Visible spectroscopy confirmed the analysis of AgNPs. The spectral data for silver nanoparticles was of an absorption peak of 420 nm which was indicative of silver SPR (Figure 1A). With longer incubation time, the absorption peak increased. This indicates that silver nanoparticles increase was of greater volume. The SPR peak was of highest and optimal width which confirmed the silver nanoparticles were of monodisperse distribution and of uniform size. For all the control assays, there was no MRS broth colour change and there was no bacterial supernatant SPR peak which confirmed the control assays the MRS broth and supernatants were void of the bacterial metabolites which confirmed the bacterial metabolite were essential for the silver nanoparticles production.

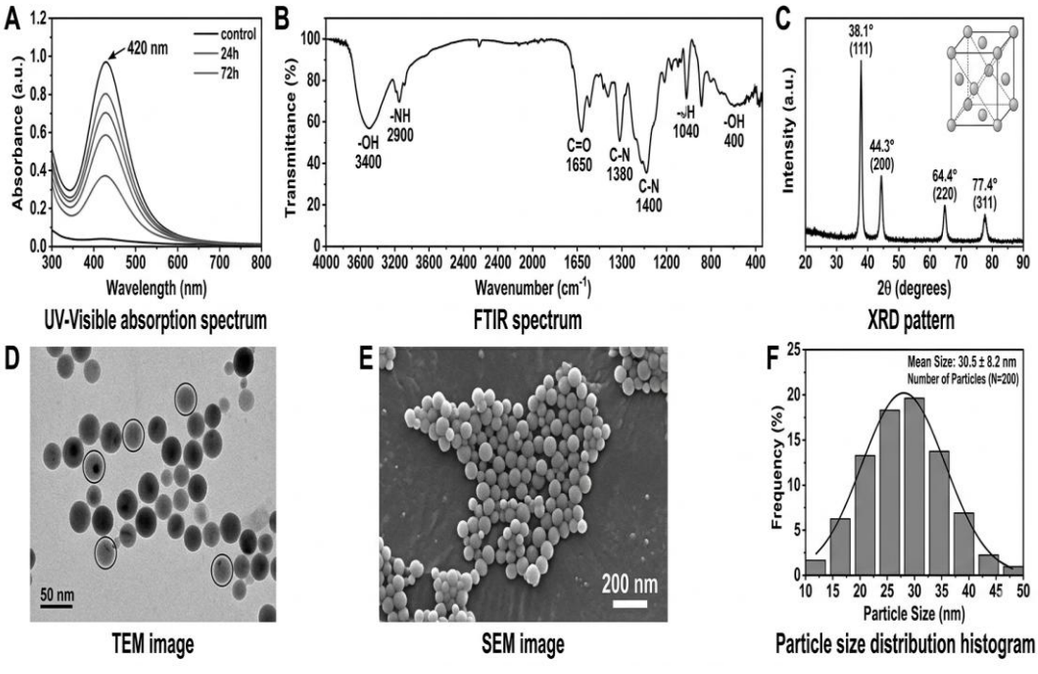

Figure -1 L. plantarum-mediated silver nanoparticles analysis. (A) UV-Visible spectrum showing peak absorption SPR absorption peak at 420 nm. (B) FTIR spectrum showing functional groups related to bioreduction and capping. (C) XRD pattern analysis showing peaks 38.1°, 44.3°, 64.4°, and 77.4° corresponding to (111), (200), (220), and (311) peaks confirming silver face-centered cubic (fcc) structure. (D) Spherical nanoparticles 15-45 nm. (E) SEM image surface morphology and distribution. (F) Size distribution histogram acquired from TEM analysis.

3.1.2 FTIR Spectroscopy

FTIR is integral in assessing the functional groups involved in the bio reduction of Ag^{+} ions and capping/stabilization of AgNPs. From the FTIR spectrum (Figure 1B), we can see several distinct absorption bands. The broad band at 3420 cm^{-1} is associated with O-H stretching vibrations (hydroxyl

groups) and N-H stretching (amines)—suggestive of proteins and polysaccharides. The band at 2925 cm^{-1} is due to C-H stretching from aliphatic chains. The prominent peak at 1635 cm^{-1} is associated with the amide I band (C=O stretching of the peptide bond) and the band at 1540 cm^{-1} is due to amide II (N-H bending and C-N stretching). The peak at 1385 cm^{-1} is due to bending of C-H from methyl groups while the bands at 1075 cm^{-1} and 1040 cm^{-1} are associated with C-O stretching (carbohydrates) and C-N stretching (amines), respectively. These functional groups from proteins, enzymes, and organic acids in the bacterial supernatant, are critical to the reduction of Ag^{+} ions and capping/stabilization of AgNPs.

3.1.3 XRD Analysis

XRD analysis shows that silver nanoparticles are present in a crystalline form. The AgNPs diffraction pattern has four crystalline peaks as shown in Figure 1C. Peaks located at 2\theta values of 38.1°, 44.3°, 64.4°, and 77.4° correspond to (111), (200), (220), and (311) planes in the face centered cubic (fcc) structure of silver (JCPDS file No. 04-0783). The highest intensity peak is the (111) peak suggesting the preferential growth of the crystal along that plane. The average crystallite size is calculated from the (111) peak using the Sherrer equation and is found to be 18 nm. The presence of sharp peaks and absence of other peaks confirms high crystallinity of the material. The absence of other peaks shows that the synthesized AgNPs has high purity and minimal contamination from other crystalline phases.

3.1.4 TEM and SEM Examination

The Transmission Electron Micrography (TEM) characterization for these AgNPs shows that they were mostly spherical with even and smooth surfaces and a minimal amount of clustering (Figure 1D). Analysis of a random sample of AgNPs (n=200) was conducted and the size distribution was determined within the range of 15 to 45 nm and averaged 28.4 ± 6.8 nm (Figure 1F). Size distribution was noted to be relatively narrow for the range of 20 to 35 nm where ~ 68% of the sample was located. The Selective Area Electron Diffraction (SAED) patterns showed crystallographic planes of (111), (200), (220), and (311) with a formation of clear rings. SAED results correspond to and further verify the results from X-ray Diffraction (XRD) analysis confirming the polycrystalline structure of the AgNPs. Scanning Electron Micrography (SEM) characterization (Figure 1E) shows obvious dispersion of the sample nanoparticles and that the small clustering that was observed was due to the sample preparation being a dry mount.

3.1.5 Zeta Potential

The assessment of zeta potential returned a value of -28.4 ± 2.1 mV, this value suggests that the suspension of AgNPs is stable within a colloid. A negative surface charge is attributed to proteins and organic acids which are negatively charged and adsorb to the surface of the nanoparticles. This creates enough repulsion to reduce the chance of aggregation. It is understood that zeta potential values around ± 25 mV are stable within colloidal systems. Our result indicates that the biogenic AgNPs will give colloidal stability in aqueous suspension for long periods of time.

3.2 Isolation of Clinical Bacterial Specimens

Fifty clinical specimens were examined and each yielded a different isolate bacterium as listed in Table 1. The most frequently isolated bacterium was Escherichia coli (32%; n=16) followed by Klebsiella pneumoniae (24%; n=12), Staphylococcus aureus (20%; n=10), Pseudomonas aeruginosa (16%; n=8) and Shigella spp. (8%; n=4) The Gram-negative bacterial isolates were in concordance with the epidemiological data concerning geographical location of healthcare-associated infections in this study.

Of the specimens collected, urinary tract infection specimens yielded the highest number of isolates followed by wound infections (30%), blood stream infections (20%), and respiratory tract infections (14%).

Table 1- Bacterial isolate distribution from clinical samples obtained from hospitals in Thi Qar Governorate, Iraq.

Bacterial Species	Number of Isolates	Percentage (%)	Sample Source Distribution
Escherichia coli	16	32.0	Urine (9), Wound (4), Blood (2), Sputum (1)
Klebsiella pneumoniae	12	24.0	Urine (5), Blood (4), Sputum (2), Wound (1)
Staphylococcus Aureus	10	20.0	Wound (6), Blood (2), Sputum (2)
Pseudomonas aeruginosa	8	16.0	Wound (4), Sputum (2), Urine (2)
Shigella spp.	4	8.0	Wound (3), Blood (1)
Total	50	100.0	Urine (18), Wound (15), Blood (10), Sputum (7)

3.3 Antimicrobial Susceptibility Profiles

Resistant to multiple drug classes and devices is alarming for multiple drug resistant organisms. Resistant strains of organisms were encountered 100% of the isolates and were resistant to 3 classes of antibiotics. Additionally, the resistance to standard antibiotics used for treatment was concerning, with the following resistance rates: ampicillin 94%, ceftriaxone 86%, ceftazidime 78%, ciprofloxacin 72%, and gentamicin 68%. 42% of the resistant gram-negative isolates were resistant to all carbapenems, and 42% (21 of 50) of the isolates were positive for carbapenemase by the modified Hodge test. NDM-1 was found in 12 (24%) of isolates (6 E. coli, 4 K. pneumoniae, and 2 P. aeruginosa). Of the S. aureus isolates, 70% (7 of 10) were methicillin resistant. Of the four classes of gram-negative bacilli isolates, Colistin was the most prevalent drug with 88% susceptibility. 12% of isolates remained resistant to Colistin and is concerning for the clinical scenario.

Table 2- Profiles of antimicrobial resistance in clinical isolates

Antibiotic	**E. coli *(n=16)***	**K. pneumoniae *(n=12)***	**S. aureus *(n=10)***	**P. aeruginosa *(n=8)***	**Shigella *spp. (n=4)***	***Overall Resistance (%)***
Ampicillin	15 (93.8%)	12 (100%)	9 (90.0%)	7 (87.5%)	4 (100%)	94.0
Amoxicillin-clavulanic acid	13 (81.3%)	10 (83.3%)	7 (70.0%)	6 (75.0%)	3 (75.0%)	78.0
Ceftriaxone	14 (87.5%)	11 (91.7%)	6 (60.0%)	7 (87.5%)	4 (100%)	84.0
Ceftazidime	12 (75.0%)	10 (83.3%)	5 (50.0%)	7 (87.5%)	3 (75.0%)	74.0
Ciprofloxacin	11 (68.8%)	9 (75.0%)	7 (70.0%)	6 (75.0%)	3 (75.0%)	72.0
Levofloxacin	10 (62.5%)	8 (66.7%)	6 (60.0%)	5 (62.5%)	2 (50.0%)	62.0
Gentamicin	11 (68.8%)	8 (66.7%)	6 (60.0%)	6 (75.0%)	3 (75.0%)	68.0
Amikacin	7 (43.8%)	6 (50.0%)	4 (40.0%)	5 (62.5%)	2 (50.0%)	48.0

Imipenem	7 (43.8%)	6 (50.0%)	N/A	4 (50.0%)	2 (50.0%)	44.2*
Meropenem	6 (37.5%)	5 (41.7%)	N/A	4 (50.0%)	2 (50.0%)	39.5*
Colistin	2 (12.5%)	2 (16.7%)	N/A	2 (25.0%)	0 (0%)	14.0*
Methicillin	N/A	N/A	7 (70.0%)	N/A	N/A	70.0**

*Percentage computed for Gram-negative isolates only (n=40)
**Percentage computed for S. aureus isolates only (n=10)
N/A: Not applicable

3.4 MIC and MBC of AgNPs

Inhibition concentration and bacterial lethality concentration of AgNPs against L. plantarum, expressed in multidrug-resistant clinical isolate studies, were determined. As in Table 3, the antimicrobial effectiveness of AgNPs was characterized from high to low activity, range of activity AgNPs was recorded; potent activity against all test organisms was noted. For Gram-negative bacteria, minimum inhibitory concentration ranged from 3.125 to 25 µg/mL, minimum bactericidal concentration ranged from 6.25 to 50 µg/mL.

S. aureus, a Gram positive bacterium, was noted to be the most susceptible of all the test organisms, where the range of minimum inhibitory concentration was 3.125 to 6.25 µg/mL and the range of minimum bactericidal concentration was 6.25 to 12.5 µg/mL. As for Gram-negative bacteria, E. coli and Shigella spp. were noted to have minimum inhibitory concentration of 6.25 to 12.5 µg/mL, while K. pneumoniae and P. aeruginosa possessed the highest MIC values noted to be 12.5 to 25 µg/mL; a high concentration was attributed to a most likely possessed more complex structure of cell wall, due to either more convoluted structure of Shigella spp. And E. coli, or due to more pronounced, structurally complex associated efflux mechanism. The NDM-1 producing isolates appeared to have the same cellular structural characteristics of other isolates, and, similar to other non-NDM-1 isolates, were noted to have MIC values of a single dilution step, suggesting that AgNPs were breaking into the associated mechanisms of carbapenemase activity. The calculated MBC/MIC ratios of 2 to 4 were a clear indication of the concentration AgNPs possessed, and it was noted that the K. pneumoniae and P. aeruginosa isolates possessed a high concentration of AgNPs, that were attributed to the predominant bactericidal activity of the AgNPs and not a mere bacteriostatic effect .

Table 3- MIC and MBC values of AgNPs for the tested MDR clinical isolates.

Bacterial Species	***Number of Isolates***	***MIC Range (µg/mL)***	***MIC_{50} (µg/mL)***	***MIC_{90} (µg/mL)***	***MBC Range (µg/mL)***	***MBC_{50} (µg/mL)***	***MBC_{90} (µg/mL)***	***MBC/MIC Ratio***
E. coli *(non-NDM-1)*	10	6.25-12.5	6.25	12.5	12.5-25	12.5	25	2-2
E. coli *(NDM-1+)*	6	6.25-12.5	12.5	12.5	12.5-25	25	25	2-2
K. pneumoniae *(non-NDM-1)*	8	12.5-25	12.5	25	25-50	25	50	2-2
K. pneumoniae *(NDM-1+)*	4	12.5-25	25	25	25-50	50	50	2-2
S. aureus *(MSSA)*	3	3.125-6.25	3.125	6.25	6.25-12.5	6.25	12.5	2-2
S. aureus *(MRSA)*	7	3.125-6.25	6.25	6.25	6.25-12.5	12.5	12.5	2-2
P. aeruginosa *(non-NDM-1)*	6	12.5-25	12.5	25	25-50	25	50	2-2
P. aeruginosa	2	12.5-25	25	25	25-50	50	50	2-2

(NDM-1+)								
Shigella *spp.*	4	6.25-12.5	6.25	12.5	12.5-25	12.5	25	2-2

MIC_{50}: Minimum inhibitory concentration (MIC) at which fifty percent (50%) of isolates are inhibited; MIC_{90}: MIC at which ninety percent (90%) of isolates are inhibited.

3.5 Anti-Biofilm Activity

Sub-MIC concentrations of nanoparticles (AgNPs) were analyzed using the crystal violet assay shown in Table 4. Researchers found that there were statistically significant differences in the effects of AgNPs when compared to the control ($p < 0.001$) in the anti-biofilm effects and effects were concentration-dependent. For Staphylococcus aureus biofilms, AgNPs scored 89.3 ± 3.2% biofilm inhibition, while Pseudomonas aeruginosa had 62.4 ± 4.8% biofilm inhibition. These AgNPs scored biofilm inhibition between 62.4% and 89.3%. For 1/4 MIC, the AgNPs biofilm inhibition dropped to between 45.8% and 71.6%. At the 1/8 MIC concentration the biofilm inhibition also suffered and dropped to 28.5% and 52.3%. Even at 1/8 MIC, there were still significant anti-biofilm effects proving that there may be prophylactic effects at much lower concentrations than those that are needed to clear planktonic cells. The removed biofilm by AgNPs on P. aeruginosa was attributed to the disruption of polysaccharide intercellular adhesin (PIA) and disruption of quorum sensing. Pseudomonas aeruginosa, and the other complex biofilms that were produced, were made of the very dense, and robust, Polysaccharide Intercellular Adhesin materials, and rough biofilm structures and therefore needed to be at higher concentrations than the other strains to be effectively inhibited [34, 35]

Table 4- Efficacy of AgNPs against MDR Clinical Isolates Biofilm

Bacterial Species	***Number of Isolates***	***Biofilm Inhibition (%) at Different AgNP Concentrations***
1/2 MIC	1/4 MIC	1/8 MIC
E. coli	16	76.8 ± 4.5
K. pneumoniae	12	68.5 ± 5.8
S. aureus	10	89.3 ± 3.2
P. aeruginosa	8	62.4 ± 4.8
Shigella *spp.*	4	78.2 ± 4.1

Data is shown as mean ± standard deviation from three separate experiments.
All values were significantly different from untreated control ($p < 0.001$, one way ANOVA).

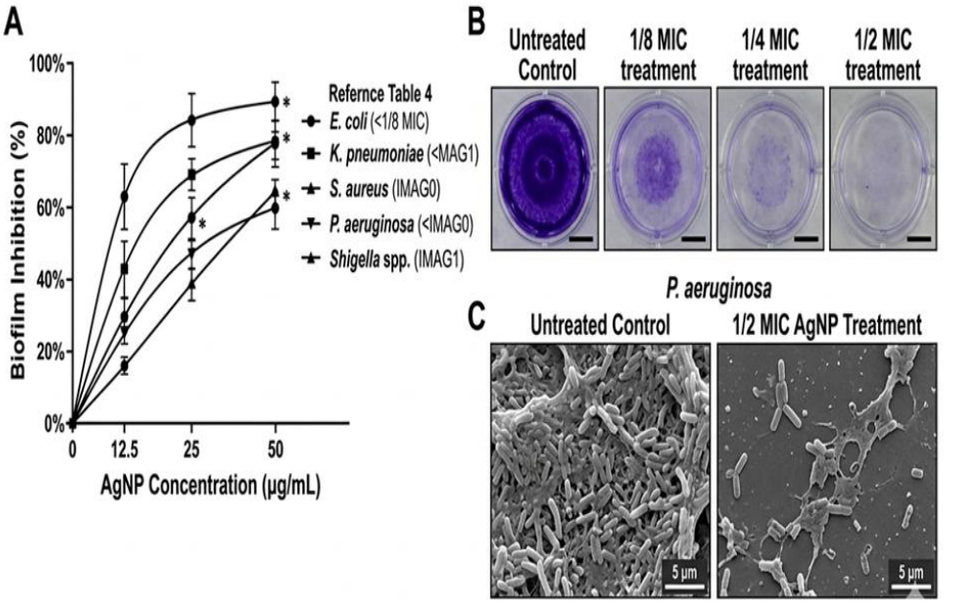

Figure -2 The anti-biofilm effect of AgNPs. (A) The dose-response curve for AgNPs as biofilm inhibitors of varying concentrations for specific bacterial strains. (B) Example of biofilm staining with crystal violet (in 96-well plates) showing the control (no AgNP treatment) and the AgNP treatment groups at 1/8 MIC, 1/4 MIC, and 1/2 MIC. (C) Scanning electron micrographs showing the difference in biofilm structure of **P. aeruginosa** in the untreated control and 1/2 MIC AgNP treated groups. The biofilm matrix was disrupted and the bacterial cells were less compared to the untreated control.

3.6 Synergistic Effects with Antibiotics

Using the checkerboard method complementary interaction between AgNPs and antibiotics was applied for the first time on MDR isolates for assessing possible positive synergistic effects. For all microorganisms tested with AgNP and ciprofloxacin combinations, Minimum Fractional Inhibitory Concentration (FIC) indices were positive for synergy and ranged from ≥ 0.18 to 0.42. Escherichia coli (FIC 0.18-0.25) and Staphylococcus aureus (FIC 0.20-0.28) showed the strongest synergy of all the tested microorganisms and with these combinations the MIC of both agents was decreased by 4-8-fold. With a range FIC index of 0.28 to 0.42, Klebsiella pneumoniae, and Pseudomonas aeruginosa showed moderate synergy. Combination of AgNP and ampicillin showed FIC of 0.25 to 0.50 indicating positive synergistic and additive effects. In the cases of ampicillin-resistant isolates, the presence of AgNPs significantly increased the susceptibility of ampicillin, lowering MIC from > 256 µg/mL to 16-64 µg/mL, which indicates that AgNPs may disrupt beta-lactamase or increase membrane permeability and assist in the diffusion of antibiotics.

Table 5- Synergistic Impact of Antibiotics and AgNPs on MDR Clinical Isolates.

Bacterial Isolate	***AgNP + Ciprofloxacin***	***AgNP + Ampicillin***
FIC Index	**Interpretation**	**MIC Reduction (fold)**
E. coli *EC-07 (NDM-1+)*	0.18	Synergy
E. coli *EC-12*	0.25	Synergy
K. pneumoniae *KP-04 (NDM-1+)*	0.28	Synergy
K. pneumoniae *KP-09*	0.35	Synergy
S. aureus *SA-03 (MRSA)*	0.20	Synergy

S. aureus *SA-08 (MRSA)*	0.28	Synergy
P. aeruginosa *PA-02 (NDM-1+)*	0.37	Synergy
**P. aeruginosa* PA-06*	0.42	Synergy
**Shigella* SH-02*	0.23	Synergy

FIC Index: Fractional Inhibitory Concentration Index; CIP: Ciprofloxacin; AMP: Ampicillin Synergy: FIC ≤ 0.5; Additive: 0.5 < FIC ≤ 1.0; Indifference: 1.0 < FIC ≤ 4.0; Antagonism: FIC > 4.0.

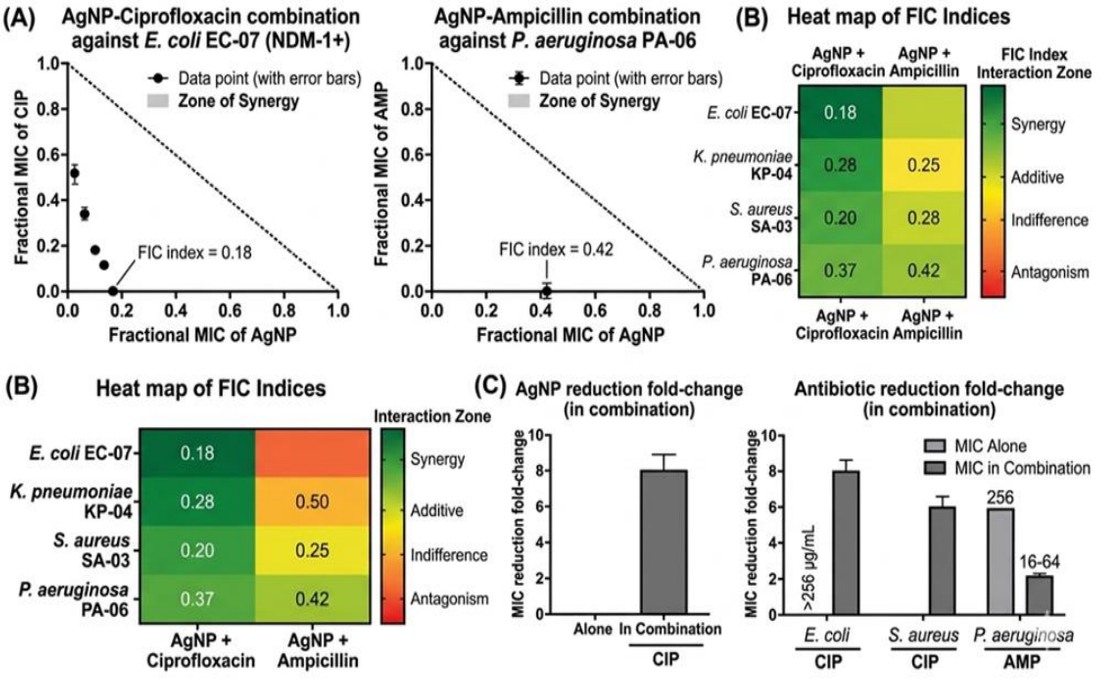

Figure -3 Synergism between AgNPs and antibiotics. (A) Isobologram plots showing synergism (data points below the line of additivity) for AgNP-ciprofloxacin and AgNP-ampicillin combinations for the treatment of representative MDR isolates. (B) Heat map representation of the FIC index for different species of bacteria and antibiotic combinations. (C) MIC reduction fold-changes of AgNPs and antibiotics used in combination compared to used alone.

3.7 Cytotoxicity Evaluation

To estimate the biocompatibility and therapeutic index, Human Dermal Fibroblast (HDF) cell cytotoxicity and the effects of silver nanoparticles (AgNPs) were assessed using the MTT assay (Table 6, Figure 4). As AgNPs concentration increased, the cytotoxicity increased, and the cells had less of a hypertoxic effect. At a concentration of 25 µg/mL and less, cell viability was over 80%. Cell viability was 68.4 ± 4.2% at 50 µg/mL and 42.7 ± 3.8% at 100 µg/mL. The IC_{50} value was 78.6 ± 5.3 µg/mL. When compared with the IC values of the bacterial pathogens, this value was 3.1 to 25.2 times greater than the corresponding minimum inhibitory concentration (MIC) value (3.125-25 µg/mL). Therefore, a good selectivity index was confirmed. The therapeutic index confirmed that AgNPs could kill bacterial pathogens while minimizing the toxicity to mammalian cells. Therefore, AgNPs can potentially be used for systemic and dermal applications. The observed cytotoxicity at these concentrations of AgNPs has been explained as due to the AgNPs inducing oxidative stress and damaging membranes of cells, tissues, and mitochondria.

Table 6- AgNPs' Cytotoxicity towards Human Dermal Fibroblast (HDF) Cells

AgNP Concentration (µg/mL)	*Cell Viability (%)*	*Standard Deviation (±)*
0 (Control)	100.0	0.0
3.125	97.8	2.1
6.25	95.3	2.8
12.5	91.6	3.4
25	84.2	3.9
50	68.4	4.2
100	42.7	3.8
200	18.5	2.9
IC_{50}	**78.6 µg/mL**	**±5.3**

Data displayed as mean ± standard deviation of three independent experiments
IC_{50}: Half-maximal inhibitory concentration determined by non-linear regression analysis.

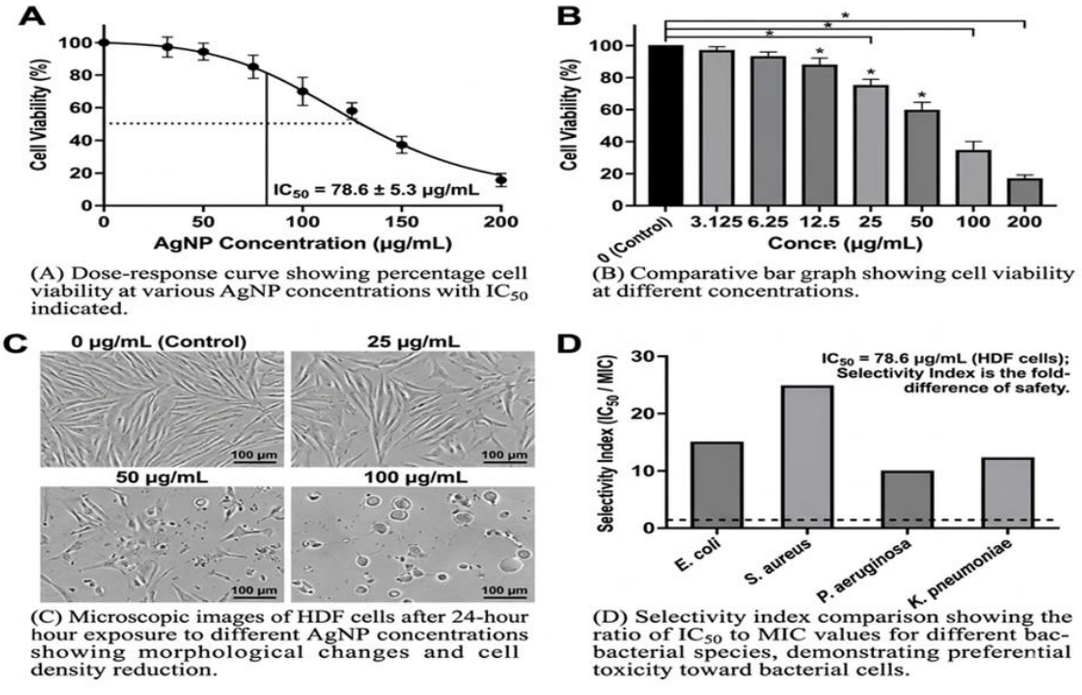

Figure -4 Assessment of cytotoxicity of AgNPs on HDF cells. (A) Shows the dose-response curve and the IC_{50} (half maximal inhibitory concentration) for cell death. (B) Shows cell viability at each concentration in a bar graph for visual representation of cell death. (C) Shows HDF cells and the morphologic changes as well as the density cell death as a function of 24 hours of exposure at (0, 25, 50, 100 µg/mL) AgNPs. (D) Shows the selectivity index with IC_{50} and MIC (Minimum inhibitory concentration) for each of the bacterial species. The selectivity index therefore shows the toxicity of the AgNPs more so on bacteria.

3.8 Molecular Docking Studies

These molecular docking studies attempt to show how AgNPs could form different types of interactions along the various proteins exposed on the bacterial membrane (Table 6, Figure 4). During the docking studies, the Ag_{13} cluster proteins showed notable binding affinity to the target proteins. Binding membrane protein of Escherichia coli, OmpA, demonstrated a binding energy of -7.8 kcal/mol with hydrogen bond interactions to amino acid residues Arg82, Asp85, and Gly135 with additional hydrophobic interactions to residues Phe17, Trp57, and Trp143. Given these interactions, AgNPs are likely to interact with the OmpA protein and rearrange membrane proteins, and increase the permeability of the membrane which could lead to bacterial cell death. For penicillin-binding protein 2a (PBP2a) of

Staphylococcus aureus, the docking study has revealed a binding energy of -8.4 kcal/mol, which is the most negative energy value obtained for the proteins studied. The main binding interactions are hydrogen bond with Ser403, Lys406, and Thr600, also a π-π stacking interaction with Tyr446 of PBP2a. The binding energy estimate to PBP2a is probably the reason for the AgNPs uptake disruption of the synthesis of the peptidoglycan layer, which is the cell wall of the bacteria and is responsible for the observed synergy with the beta-lactam antibiotics. For the case of the outer membrane protein F (Opr F) of Pseudomonas aeruginosa, the binding energy is -6.8 kcal/mol arising due to the interaction from residues Arg58, Asp97, and Tyr121.The binding energy, demonstrated in P. aeruginosa, explains the increased MIC values seen in this organism, reflecting a more resistant phenotype .

Table 7- Results of molecular docking of AgNPs and bacterial membrane proteins.

Target Protein	*Bacterial Species*	*PDB ID*	*Binding Energy (kcal/mol)*	*Key Interacting Residues*	*Types of Interactions*
Outer Membrane Protein A (OmpA)	**E. coli**	1QJP	**-7.8**	Arg82, Asp85, Gly135, Phe17, Trp57, Trp143	H-bonds, hydrophobic, π-π stacking
Penicillin-Binding Protein 2a (PBP2a)	**S. aureus**	3ZG0	**-8.4**	Ser403, Lys406, Thr600, Tyr446	H-bonds, π-π stacking, electrostatic
Outer Membrane Porin F (OprF)	**P. aeruginosa**	2LHF	**-6.8**	Arg58, Asp97, Tyr121	H-bonds, electrostatic

H-bonds: Hydrogen bonds

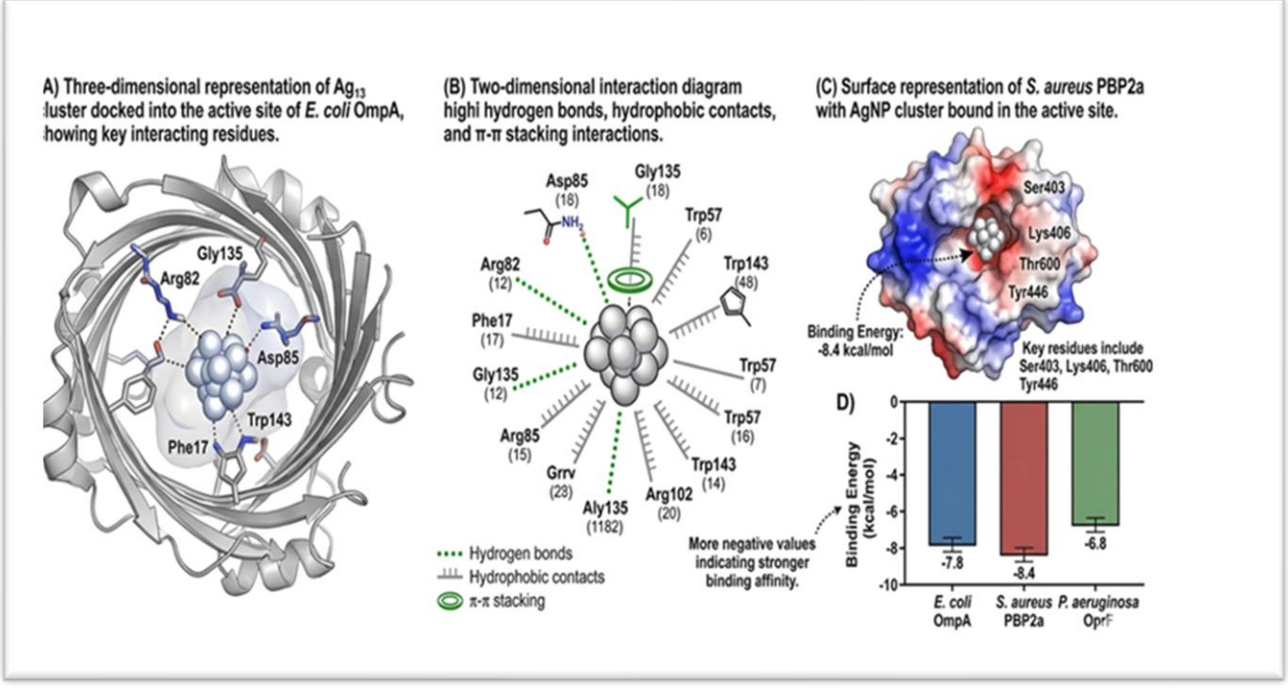

Figure -5 Analysis of molecular docking of proteins and silver nanoparticles (AgNPs). (A) 3D model of docked Ag_{13} cluster to the active site of E. coli OmpA with interacting residues. (B) Interaction diagram with hydrogen bonds, hydrophobic interactions, and π-π stacking contacts. (C) Surface model of S. aureus PBP2a with AgNP cluster in the active site. (D) Binding energy comparison in a bar graph for various target proteins where more negative values indicate higher binding affinity.

4. Discussion

This study sheds light on the antimicrobial activity of silver nanoparticles synthesized using Lactobacillus plantarum; the study focused on the clinically isolated multidrug-resistant pathogens from Thi Qar Governorate, Iraq, during the limited antimicrobial resistance (AMR) studies in the southern parts of Iraq. The successful green synthesis of silver nanoparticles using the supernatant of Lactobacillus plantarum is an exceptional case for an eco-friendly, non-toxic, biocompatible, sustainable, and cost-effective method for silver nanoparticles production [16, 36]

The silver nanoparticles obtained from Lactobacillus plantarum showed morphological and dimensional uniformity confirmed by a unique surface plasmon resonance (SPR) peak at 420 nm in UV-Vis spectroscopy in tandem with previous studies on Lactobacillus plantarum [21]. A peak absorption intensity increase after 72 hours indicates the bio reduction of Ag^{+} ions by biological reductants present in the supernatant (NADH-dependent reductases, lactic and acetic acid [organic acids], extracellular proteins), .Protenas and the organic acids were confirmed by FTIR as capping and reductants .The peaks due to amide bonds of proteins and the hydroxyl groups responsible for the stabilization of nanoparticles were observed at 1635 cm^{-1}, 1540 cm^{-1}, and 3420 cm^{-1}, respectively[37]. The X-ray diffraction (XRD) studies show that AgNPs have a crystalline structure with the typical face-centered cubic (fcc) silver peaks and a crystallite size of 18 nm evaluated from the Scherrer equation, which is consistent with the optimum size for nanoparticles to exhibit antimicrobial activity. Nanoparticles in the size range of 10-50 nm have been reported to enhance cellular uptake and interaction with bacterial membranes which improves antimicrobial activity [24, 38, 39].

The spherical nanoparticles identified via transmission electron microscopy (TEM) were found to be in the size range of 15-45 nm (28.4 nm average). Antimicrobial activity is expected from these nanoparticles. When explaining the variance in size from X-ray diffraction (XRD) data which gives a crystallite size of 18 nm and TEM data of 28.4 nm, it is important to note that the range of XRD is small, confined to few coherent diffracting crystalline domains, whereas TEM is measuring the particle size which includes amorphous materials and any possible capping layers. A value of -28.4 mV zeta potential shows good stability of the colloid, and in this case, stability comes from the electrostatic repulsion from the aggregated biomolecules that have a negative charge on the surface of the nanoparticles. These repulsive forces prevent aggregation and offer a long lasting stability in suspension[40].

The epidemiological profile of clinical isolates from this study is an unprecedented analysis of the Iraqi healthcare system and multidrug resistance detailing concerning levels of 100% of the isolates being classified as multidrug- resistant (MDR) with 42% being carbapenem resistant. The presence of NDM-1 genes in 24% of the isolates is worrisome as NDM-1 producing organisms are very resistant to almost all β- lactam antibiotics including carbapenems and are also capable of acquiring and readily disseminating antibiotic resistance through horizontal gene transfer making them extremely dangerous. The prevalence of methicillin-resistant Staphylococcus aureus (MRSA) is 70% which confirms further the necessity to direct research to modern antimicrobial techniques[41, 42].

The AgNPs synthesized using L. plantarum show an antimicrobial efficacy with an MIC value of 3.125 to 25 μg/mL, proving to be effective and equal to or even better than efficacy of biogenic AgNPs previously reported [27, 43] .It is of interest that the microbicidal effect for the tested NDM-1 positive and NDM-1 negative isolates is the same and suggests that AgNPs are able to break down the antimicrobial activity associated with carbapenemases as this is a result of their antimicrobial activity which is not coupled with activity of any enzymatic resistance [44].AgNPs are known for their antimicrobial activity for various reasons. The range of 2 to 4 for the MBC/MIC ratios implies membrane disruption, oxidative damage to the lipids, proteins, DNA, and the so-called primary ROS, which is described as damaging activity related to mitochondrial dysfunction [12].The antimicrobial activity of AgNPs is the most versatile. Regarding the susceptibility of bacteria to AgNPs, it varies for Gram-positive and Gram-

negative. Staphylococcus aureus is the Gram-positive species with the lowest MIC values (3.125-6.25 μg/mL), which is due to the nature of the cell envelope. As a result, due to the assumed ease of penetration of AgNPs[45], the relatively thick peptidoglycan layer of Gram-positive bacteria is more conducive compared to the outer membrane that is present in Gram-negative bacteria. In contrast, this is perceived as an outer membrane structure for Gram-negative bacteria, and the slight (2-4 fold) variation in MIC values of AgNPs supports this conclusion that AgNPs can interact with lipopolysaccharides and porins [46].

It is extremely impressive that silver nanoparticles (AgNPs) exhibit pronounced anti-biofilm effects at sub-minimum inhibitory concentrations (62-89% inhibition at 1/2 MIC) given that other antibiotics have concentrations that are 100 to 1000 times higher than the MIC to achieve comparable levels of biofilm disruption[8, 10]. Anti-biofilm activities may consist of preventing initial bacterial adhesion, disrupting quorum sensing pathways, and biofilm matrix penetration and cell lysis[35]. For instance, Silver NPs (AgNPs) have anti-biofilm activity in Staphylococcus aureus (89.3% inhibition) due to the inhibition of polysaccharide intercellular adherent (PIA) and the agr quorum sensing system[23]. In addition, AgNPs have shown possible synergistic effects and strategies against pathogens in the biofilm state due to their anti-biofilm activity with 62.4% inhibition at 1/2 MIC against Pseudomonas aeruginosa, which is a notorious biofilm former with multiple mechanisms of resistance[47].

The positive interactions seen in this study between silver nanoparticles (AgNPs) and typical antibiotics (ciprofloxacin and ampicillin) with FIC values between 0.18 and 0.50, confirm the efficacy for combination therapy. These interactions function through different mechanisms, such as enhancement of membrane permeability by AgNPs, which fosters antibiotic penetration, inhibits antibiotic efflux pumps, generates reactive oxygen species (ROS) that further damage antibiotics and disrupts resistance mechanisms that include β-lactamases[13, 14, 41]. AgNPs restoring the efficacy of ampicillin against resistant isolates is significant, which illustrates the ability of AgNPs to preserve β-lactam antibiotics from enzymatic degradation and/or improve accessibility of the antibiotics to the desired site of action. This is consistent with the molecular docking studies which showed AgNPs having a good binding affinity to PBP2a, thereby potentially altering the activity of PBP2a and making β-lactam antibiotic coated bacteria susceptible[48].

HDF cells showed IC50 of 78.6 µg/mL which is 3.1-25.2 fold larger than the MIC of the bacterial pathogens investigated. This shows a good selective index. With respect to the differences between prokaryotes and eukaryotes, biosafety level 2 is considered acceptable. These differences include the absence of a cell wall in mammals, differences in the lipids of the membranes and eukaryotes having a more advanced antioxidant system[42, 49]. Above 50 µg/mL, effects from calcium imbalance, oxidative stress, and apoptosis, which are also described elsewhere, are the main cytotoxic effects[50]. These positive effects still advocate the use of topical formulations of silver nanoparticles (Ag NPs) for the management of infected wounds, and after some modifications, the use of them systemically could also be possible[7].

The use of Molecular Docking explained various mechanistic interactions of AgNPs and bacteria at a molecular level. This showed that AgNPs can attack and modify vital structural proteins that sustain life in bacteria. Most of the bacterial membrane proteins that AgNPs can bind to and modify sustain life in bacteria. and sustain life in bacteria. This study confirms that AgNPs have multiple sites of action with the most negative binding affinity (−8.4 kcal/mol) to S. aureus PBP2a and most positive MICs with respect to S. aureus. Most negative MIC values of S. aureus confirms most spread synergistic molecular action when used in combination with β-lactam antibiotics. This study shows that AgNPs modify outer membrane permeability to give bacteria an increased ability to uptake antibiotics or other anti-bacterial substances [51].

This study provides a holistic view of L. plantarum synthesizing silver nanoparticles (AgNPs) as antimicrobial agents incorporating eco- friendly synthesis, wide-ranging characterization, exhaustive microbiological testing, and in silico studies. Considering the findings, the apprehensions in the clinical

context regarding the rapid spread of multi-drug resistance (MDR) especially for topical wound management, catheter coating, sterilization of instruments, and systemic applications with antibiotics, are warranted[52, 53]. However, a number of limitations should be noted. The first and most important limitation is that this study was entirely in vitro, and further research is needed in animal models and clinical studies to evaluate in vivo effectiveness, biodistribution, and toxicity of the AgNPs. The second important limitation is the resistance mechanisms that could emerge to counter AgNPs, and the complexity of this issue may be underestimated and, therefore, careful study and oversight are needed for long periods. The third important limitation is the use of AgNPs and their impact on the health of microbiota, beneficial microorganisms and the various ecosystems that support microbiota.
Subsequent studies should focus on in vivo studies with animal infection models, the effects of AgNPs on polymicrobial biofilms and the host immune system, innovative targeted delivery systems to improve bioavailability and reduce off-target toxicity, possible synergistic effects with other antimicrobials and immunomodulators, and the assessment of the environmental biodegradation and ecological effects of AgNPs. Also, to move these promising results from in vitro studies into practice, the research on the safety and efficacy of AgNPs in humans should be conducted.

5. Conclusion

The current study investigates Lactobacillus plantarum and silver nanoparticles (AgNPs) as possible options to counter the problems multi-drug resistant infections from clinical isolates in the Thi Qar Governorate of Iraq. The integration of these two components provides an innovative and inexpensive approach to the generation of homogeneous nanoparticles and AgNPs, which holds great potential for antimicrobial uses. The generated AgNPs have high bactericidal activity against a variety of multi-drug resistant pathogens, including NDM-1 producing strains, and have anti-biofilm activity as well as synergistic sub-inhibitory concentrations with antibiotics to restore antibiotic activity against resistant strains with a positive selectivity index. Molecular docking studies, which provide an understanding of the AgNPs and bacteria interactions, showed that AgNPs have a strong binding affinity to one or more bacterial membrane proteins, proving that these nanoparticles are excellent candidates for biogenic AgNPs. AgNPs are considered to be excellent biogenic candidates due to their antimicrobial activity and good selectivity, which means that they can be used in biogenic AgNPs designed to treat wounds or be used in biogenic AgNPs for coated medical devices. However, it is necessary to perform studies to evaluate the in vivo clinical efficacy of these biogenic AgNPs, particularly with respect to their use as coated devices. The combination of both probiotics and bioactive nanoparticles with bacterial resistance mechanisms is, in general, an excellent approach to biotechnologically address the problems of antimicrobial resistant microbes and antigen-resistant pathogens due to the mechanisms of inhibition, destruction, and regulation of the pathogenic microbes.

Acknowledgments

All personnel involved at Al-Hussein Teaching Hospital, and Al-Nasiriyah General Hospital located in Thi Qar Governorate of Iraq, and University of Sumer in Iraq, deserve our appreciation for their contribution in obtaining the clinical samples and providing us with the technical support and the laboratory services, as well as the participants for this research study.

Conflict of Interest

The authors of this research have no conflicts of interest to declare.

Funding

This research did not receive any funding from public, commercial, or not-for-profit agencies.

Reference

[1] A. Algburi, R. M. Mubarak, T. H. Mubarak, S. Fathi-karkan, A. Rahdar, and L. F. Romanholo Ferreira, "Lactobacillus acidophilus and mixed probiotic-mediated synthesis of silver nanoparticles: Antibacterial efficacy against multidrug-resistant otopathogens," *BioNanoScience*, vol. 15, no. 3, p. 419, 2025.

[2] E. Khalifa, M. Abdel Rafea, N. Mustapha, R. Sultan, and E. Hafez, "Silver nanoparticles synthesized by probiotic bacteria and antibacterial role in resistant bacteria," *AMB Express*, vol. 13, no. 1, p. 140, 2023.

[3] M. S. Ayubee *et al.*, "Synergistic antibacterial action of AgNP-ampicillin conjugates: Evading β-lactamase degradation in ampicillin-resistant clinical isolates," *Plos one*, vol. 20, no. 9, p. e0331669, 2025.

[4] E. M. Desouky, M. A. Shalaby, M. K. Gohar, and M. A. Gerges, "Evaluation of antibacterial activity of silver nanoparticles against multidrug-resistant gram negative bacilli clinical isolates from Zagazig University hospitals," *Microbes and Infectious Diseases*, vol. 1, no. 1, pp. 15–23, 2020.

[5] I. J. Naser, "Enhancement of anti-bactericidal and anti-biofilm activities of silver nanoparticles against multidrug-resistant enteric pathogens isolated from children with diarrhea," *Journal of Biotechnology Research Center*, vol. 16, no. 2, 2022.

[6] S. H. Haji, F. A. Ali, and S. T. H. Aka, "Synergistic antibacterial activity of silver nanoparticles biosynthesized by carbapenem-resistant Gram-negative bacilli," *Scientific Reports*, vol. 12, no. 1, p. 15254, 2022.

[7] M. Muddassir *et al.*, "Antibacterial efficacy of silver nanoparticles (AgNPs) against metallo-β-lactamase and extended spectrum β-lactamase producing clinically procured isolates of Pseudomonas aeruginosa," *Scientific reports*, vol. 12, no. 1, p. 20685, 2022.

[8] S. Gurunathan, J. W. Han, D.-N. Kwon, and J.-H. Kim, "Enhanced antibacterial and anti-biofilm activities of silver nanoparticles against Gram-negative and Gram-positive bacteria," *Nanoscale research letters*, vol. 9, no. 1, p. 373, 2014.

[9] M. S. Tawre, A. Shiledar, S. K. Satpute, K. Ahire, S. Ghosh, and K. Pardesi, "Synergistic and antibiofilm potential of Curcuma aromatica derived silver nanoparticles in combination with antibiotics against multidrug-resistant pathogens," *Frontiers in Chemistry*, vol. 10, p. 1029056, 2022.

[10] M. Mishra, A. Ballal, D. Rath, and A. Rath, "Novel silver nanoparticle-antibiotic combinations as promising antibacterial and anti-biofilm candidates against multiple-antibiotic resistant ESKAPE microorganisms," *Colloids and Surfaces B: Biointerfaces*, vol. 236, p. 113826, 2024.

[11] E. D. Cavassin *et al.*, "Comparison of methods to detect the in vitro activity of silver nanoparticles (AgNP) against multidrug resistant bacteria," *Journal of nanobiotechnology*, vol. 13, no. 1, p. 64, 2015.

[12] D. S. Ipe, P. S. Kumar, R. M. Love, and S. M. Hamlet, "Silver nanoparticles at biocompatible dosage synergistically increases bacterial susceptibility to antibiotics," *Frontiers in microbiology*, vol. 11, p. 1074, 2020.

[13] M. Lopez-Carrizales *et al.*, "In vitro synergism of silver nanoparticles with antibiotics as an alternative treatment in multiresistant uropathogens," *Antibiotics*, vol. 7, no. 2, p. 50, 2018.

[14] M. T. Yassin, A. A.-F. Mostafa, A. A. Al-Askar, and F. O. Al-Otibi, "Synergistic antibacterial activity of green synthesized silver nanomaterials with colistin antibiotic against multidrug-resistant bacterial pathogens," *Crystals*, vol. 12, no. 8, p. 1057, 2022.

[15] H. Khan, A. Gul, Z. Najam, and T. Malik, "Biogenic silver nanoparticles optimization using Plackett–Burman design and its synergistic effect with cefotaxime against multidrug resistant clinical isolates," *Scientific Reports*, vol. 15, no. 1, p. 18742, 2025.

[16] A. Abdelgadir *et al.*, "Probiotic Lactobacillus salivarius mediated synthesis of silver nanoparticles (AgNPs-LS): A sustainable approach and multifaceted biomedical application," *Heliyon*, vol. 10, no. 18, 2024.

[17] A. S. El-Hawary, O. M. Ibrahim, M. H. Kalaba, M. H. El-Sehrawy, and M. K. Ismail, "Limosilactobacillus fermentum-derived silver nanoparticles: biosynthesis, optimization, and biological activities," *Biomass Conversion and Biorefinery*, vol. 15, no. 7, pp. 9999–10013, 2025.

[18] E. Z. Gomaa, "Synergistic antibacterial efficiency of bacteriocin and silver nanoparticles produced by probiotic Lactobacillus paracasei against multidrug resistant bacteria," *International Journal of Peptide Research and Therapeutics*, vol. 25, no. 3, pp. 1113–1125, 2019.

[19] A. A. Mohammed, A. Hegazy, and A. Salah, "Novelty of synergistic and cytotoxicity activities of silver nanoparticles produced by Lactobacillus acidophilus," *Applied Nanoscience,* vol. 13, no. 1, pp. 633–640, 2023.

[20] P. Prema *et al.*, "Microbial synthesis of silver nanoparticles using Lactobacillus plantarum for antioxidant, antibacterial activities," *Inorganic Chemistry Communications,* vol. 136, p. 109139, 2022.

[21] A. K. Ravi *et al.*, "Biosynthesis of chitosan encapsulated silver-nanoparticles using Probiotic-Lactobacillus plantarum strain and it's in vitro anticancer assessment on HeLa cells," *Medicine in Microecology,* vol. 22, p. 100117, 2024.

[22] K. Nihala, M. Mohan, P. Seena, J. Johney, and R. Ragunathan, "Fabrication and Characterization of Silver Nanoparticles Produced by the Supernatant of Lactobacillus gasseri and Evaluation of their Potential Biomedical Activity," *South Asian Journal of Research in Microbiology,* vol. 19, no. 8, pp. 39–49, 2025.

[23] M. Pourhaji, F. Abbasi, A. Sehatpour, and R. Bakhtiari, "Biological Synthesis of Silver Nanoparticles Using Lactobacillus Probiotic Bacterium and Evaluation of Their Cytotoxicity Against Oral Squamous Cell Carcinoma Cell Line: AgNPs Cytotoxicity Against Squamous Cell Carcinoma," *Galen Medical Journal,* vol. 13, p. e2905, 2023.

[24] G. Ogunleye, K. Oyinlola, A. Aguokoli, and T. Oyewo, "Silver nanoparticles from Lactobacillus Delbrueckii: Microbial synthesis, characterization and antibacterial activity," *Innovative Romanian Food Biotechnology,* no. 22, pp. 1–13, 2022.

[25] A. M. Awadelkareem *et al.*, "Biosynthesized silver nanoparticles derived from probiotic Lactobacillus rhamnosus (AgNPs-LR) targeting biofilm formation and quorum sensing-mediated virulence factors," *Antibiotics,* vol. 12, no. 6, p. 986, 2023.

[26] P. Nordmann, L. Poirel, T. R. Walsh, and D. M. Livermore, "The emerging NDM carbapenemases," *Trends in microbiology,* vol. 19, no. 12, pp. 588–595, 2011.

[27] M. Ansari *et al.*, "Evaluation of antibacterial activity of silver nanoparticles against MSSA and MSRA on isolates from skin infections," 2011.

[28] A. Dey, A. Dasgupta, V. Kumar, A. Tyagi, and A. K. Verma, "Evaluation of the of antibacterial efficacy of polyvinylpyrrolidone (PVP) and tri-sodium citrate (TSC) silver nanoparticles," *International Nano Letters,* vol. 5, no. 4, pp. 223–230, 2015.

[29] A. Barapatre, K. R. Aadil, and H. Jha, "Synergistic antibacterial and antibiofilm activity of silver nanoparticles biosynthesized by lignin-degrading fungus," *Bioresources and Bioprocessing,* vol. 3, no. 1, p. 8, 2016.

[30] S. Stepanović, D. Vuković, I. Dakić, B. Savić, and M. Švabić-Vlahović, "A modified microtiter-plate test for quantification of staphylococcal biofilm formation," *Journal of microbiological methods,* vol. 40, no. 2, pp. 175–179, 2000.

[31] F. C. Odds, "Synergy, antagonism, and what the chequerboard puts between them," vol. 52, ed: Oxford University Press, 2003, pp. 1–1.

[32] S. I. Othman and F. H. Kamel, "Bioinspired synthesis of silver nanoparticles using L. reuteri: antibacterial efficacy, molecular docking insights, and cytotoxicity assessment," *ChemistrySelect,* vol. 10, no. 2, p. e202404505, 2025.

[33] O. Trott and A. J. Olson, "AutoDock Vina: improving the speed and accuracy of docking with a new scoring function, efficient optimization, and multithreading," *Journal of computational chemistry,* vol. 31, no. 2, pp. 455–461, 2010.

[34] A. O. Adesina, "Antibacterial activity of silver-conjugated magnetic iron oxide nanoparticles," *Scholars International Journal of Chemistry and Material Sciences,* vol. 5, pp. 23–28, 2022.

[35] B. Ramalingam, T. Parandhaman, and S. K. Das, "Antibacterial effects of biosynthesized silver nanoparticles on surface ultrastructure and nanomechanical properties of gram-negative bacteria viz. Escherichia coli and Pseudomonas aeruginosa," *ACS applied materials & interfaces,* vol. 8, no. 7, pp. 4963–4976, 2016.

[36] S. Suba, S. Vijayakumar, M. Nilavukkarasi, E. Vidhya, and V. Punitha, "Eco synthesized silver nanoparticles as a next generation of nanoproduct in multidisciplinary applications," *Environmental Chemistry and Ecotoxicology,* vol. 4, pp. 13–19, 2022.

[37] S. S. Shankar, A. Rai, A. Ahmad, and M. Sastry, "Rapid synthesis of Au, Ag, and bimetallic Au core–Ag shell nanoparticles using Neem (Azadirachta indica) leaf broth," *Journal of colloid and interface science,* vol. 275, no. 2, pp. 496–502, 2004.

[38] B. Cullity and S. Stock, "Elements of X-ray Diffraction Third Edition, 2001," ed: Upper Saddle River, NJ: Prentice Hall.

[39] A.-P. Magiorakos *et al.*, "Multidrug-resistant, extensively drug-resistant and pandrug-resistant bacteria: an international expert proposal for interim standard definitions for acquired resistance," *Clinical microbiology and infection*, vol. 18, no. 3, pp. 268–281, 2012.

[40] M. A. Polinarski *et al.*, "New perspectives of using chitosan, silver, and chitosan–silver nanoparticles against multidrug-resistant bacteria," *Particle & Particle Systems Characterization*, vol. 38, no. 4, p. 2100009, 2021.

[41] M. Palau Gauthier *et al.*, "In Vitro Antibacterial Activity of Silver Nanoparticles Conjugated with Amikacin and Combined with Hyperthermia against Drug-Resistant and Biofilm-Producing Strains."

[42] P. AshaRani, G. Low Kah Mun, M. P. Hande, and S. Valiyaveettil, "Cytotoxicity and genotoxicity of silver nanoparticles in human cells," *ACS nano*, vol. 3, no. 2, pp. 279–290, 2009.

[43] K. A. A. A. Rahim and A. M. A. Mohamed, "Bactericidal and antibiotic synergistic effect of nanosilver against methicillin-resistant Staphylococcus aureus," *Jundishapur journal of microbiology*, vol. 8, no. 11, p. e25867, 2015.

[44] I. Sondi and B. Salopek-Sondi, "Silver nanoparticles as antimicrobial agent: a case study on E. coli as a model for Gram-negative bacteria," *Journal of colloid and interface science*, vol. 275, no. 1, pp. 177–182, 2004.

[45] C.-N. Lok *et al.*, "Silver nanoparticles: partial oxidation and antibacterial activities," *JBIC Journal of Biological Inorganic Chemistry*, vol. 12, no. 4, pp. 527–534, 2007.

[46] M. Otto, "Staphylococcal infections: mechanisms of biofilm maturation and detachment as critical determinants of pathogenicity," *Annual review of medicine*, vol. 64, no. 1, pp. 175–188, 2013.

[47] N. Høiby, T. Bjarnsholt, M. Givskov, S. Molin, and O. Ciofu, "Antibiotic resistance of bacterial biofilms," *International journal of antimicrobial agents*, vol. 35, no. 4, pp. 322–332, 2010.

[48] R. Foldbjerg, P. Olesen, M. Hougaard, D. A. Dang, H. J. Hoffmann, and H. Autrup, "PVP-coated silver nanoparticles and silver ions induce reactive oxygen species, apoptosis and necrosis in THP-1 monocytes," *Toxicology letters*, vol. 190, no. 2, pp. 156–162, 2009.

[49] O. O. Adeniji, M. O. Ojemaye, and A. I. Okoh, "Antibacterial activity of metallic nanoparticles against multidrug-resistant pathogens isolated from environmental samples: nanoparticles/antibiotic combination therapy and cytotoxicity study," *ACS Applied Bio Materials*, vol. 5, no. 10, pp. 4814–4826, 2022.

[50] B. Reidy, A. Haase, A. Luch, K. A. Dawson, and I. Lynch, "Mechanisms of silver nanoparticle release, transformation and toxicity: a critical review of current knowledge and recommendations for future studies and applications," *Materials*, vol. 6, no. 6, pp. 2295–2350, 2013.

[51] J. P. Ruparelia, A. K. Chatterjee, S. P. Duttagupta, and S. Mukherji, "Strain specificity in antimicrobial activity of silver and copper nanoparticles," *Acta biomaterialia*, vol. 4, no. 3, pp. 707–716, 2008.

[52] H. H. Lara, N. V. Ayala-Núñez, L. d. C. Ixtepan Turrent, and C. Rodríguez Padilla, "Bactericidal effect of silver nanoparticles against multidrug-resistant bacteria," *World Journal of Microbiology and Biotechnology*, vol. 26, no. 4, pp. 615–621, 2010.

[53] B. B. Hair, M. E. Conley, T. M. Wienclaw, M. J. Conley, and B. K. Berges, "Synergistic activity of silver nanoparticles and vancomycin against a spectrum of Staphylococcus aureus biofilm types," *BioRxiv*, p. 337436, 2018.